

Seismic Behaviour of Steel Wide-Flange Columns in Ductile Moment-Resisting Frames Considering Base Plate Flexibility



Omid Moammer, Ali Imanpour, and Robert Tremblay

Abstract This paper aims to examine the seismic behaviour of steel wide-flange columns in steel ductile moment-resisting frames considering the deformations of the base plate and anchor rods. A prototype MRF is first designed in accordance with the Canadian steel design standard (CSA S16-19) seismic provisions. A continuum finite element model of the interior first-storey column isolated from the prototype frame is then developed together with the base footing and connection. The flexibility of the adjoining beams at the top end of the column is also considered in the numerical model. The capability of the model components in reproducing the cyclic response of the wide-flange column and its base conditions are then calibrated against available experimental test data. Special attention is placed on the cyclic response of the anchor rods and base plate. The seismic response of the columns of the prototype frame is finally examined using the corroborating finite element model under realistic seismic demands obtained from the two-dimensional concentrated plasticity-based numerical model of the frame subjected to representative earthquake ground motions. The results from the finite element analyses confirm that base flexibility can influence the inelastic cyclic response and the stability of first-storey MRF columns. Furthermore, the proposed numerical modelling technique can be used in future studies to properly simulate the inelastic seismic response of the column base plate, anchor rods, and footing for the purpose of MRF response evaluation.

Keywords Wide-flange columns · Steel moment-resisting frames · Nonlinear modelling · Seismic behaviour · Base flexibility

O. Moammer (✉) · A. Imanpour

Department of Civil and Environmental Engineering, University of Alberta, Edmonton, AB, Canada

e-mail: moammer@ualberta.ca

R. Tremblay

Department of Civil, Geological and Mining Engineering, Polytechnique Montréal, Montreal, QC, Canada

© Canadian Society for Civil Engineering 2023

R. Gupta et al. (eds.), *Proceedings of the Canadian Society of Civil Engineering*

Annual Conference 2022, Lecture Notes in Civil Engineering 348,

https://doi.org/10.1007/978-3-031-34159-5_17

1 Introduction

Steel moment-resisting frames (MRFs) are used commonly as a lateral load-resisting system of multi-storey buildings in high-seismic areas. MRFs, in particular those part of low- and mid-rise buildings, are made of wide-flange beams and columns. In Canadian design practice, the MRF column base connections include embedded and exposed connections. Embedded base connections are ideally considered to be fixed and are suitable for mid-rise and high-rise buildings with relatively large columns. Exposed column base connections act as a suitable and economical solution for low- and mid-rise buildings in which bending moments at the column bases are relatively lower. Greater rotational flexibility is expected in exposed column base connections compared to their embedded counterpart, which suggests that they cannot be considered as fully restrained in analysis and design [30]. Past experimental studies and post-earthquake observations confirmed that column base connections can influence the seismic performance of MRF columns and, in turn, the system [2, 4, 9, 13, 15, 28, 33, 34]. Furthermore, analytical studies performed on MRF base connections showed that base flexibility can affect the plastic mechanism of the structure, affecting ductility, strength, seismic demand, and stability [22, 36].

Exposed column base connections have been the subject of extensive research in the past. References [9, 15, 33] studied experimentally the seismic response of exposed base connections under axial load and strong axis bending. The observed failure modes included plate yielding, anchor rod yielding, weld fracture, and crushing of grout. Lee et al. [24] investigated the influence of weak axis bending on the base connection response using numerical simulations and showed that ratio between the strength of the column, base plate, anchor rods, and grout controls the response of the connection. Lee et al. [25] tested four specimens under cyclic loading history and reported cracks at the column flange tips after 1% drift, which had unnoticeable influence on strength degradation, even up to 5% drift. Choi et al. [7] studied the effect of biaxial bending on the seismic behaviour of column base connections using six square hollow structural section (HSS) specimens. The results confirmed the occurrence of pinching behaviour owing to anchor rod yielding when thick base plate was used, and due to base plate yielding in the case of thin base plate. Bajer et al. [3] studied experimentally and numerically four base connections under biaxial and uniaxial bending conditions in the presence of a constant axial compression load. The observed failure modes for the specimens under biaxial bending and axial load involved anchor rod rupture at around 10% drift. Seco et al. [31] investigated experimentally the effect of the base plate thickness and axis of bending on the performance of column base connections and reported anchor rod and base plate yielding as the observed failure modes. A total of 32 column base specimens were tested under biaxial bending and axial compression to provide insight into the effect of the base plate thickness, anchor rod diameter, and axial force level on the failure modes as well as strength and stiffness of exposed base column connections [8]. Pan et al. [30] studied six specimens with four internal anchor bolts representing a pinned base column connection under strong and weak axis bending and showed that under

strong axis bending punching shear failure of the column flanges and anchor rods governed the behaviour, whereas anchor rod pullout dominated the response in the specimens under weak axis bending.

Extensive research effort has been put in the past decade to study the cyclic response of wide-flange steel columns located in the first storey of MRFs with base plastic hinging [12, 35]. In these test programs, the flexibility of the base connection was ignored, although some of these specimens were tested taking into account the flexibility provided by the storey beam [11, 12, 35]. It was shown in other test programs that the flexibility of the column base connection can affect the column failure mode and the amplitude of column axial shortening, which in turn affects the column seismic stability [10, 20]. The evaluation of the seismic response of embedded base connections showed that they possess limited inherent flexibility although cracks were observed in concrete base. The evaluation of the interaction between steel wide-flange MRF columns and their embedded base connections showed that base flexibility can lead to a more satisfactory seismic response by delaying the formation of plastic hinges at the column bases [18–20].

Although the nonlinear response and stability of wide-flange steel columns under seismic load effects have been investigated extensively in the past, the influence of the deformations occurring in column base connections including the base plate, anchor rods, and concrete footing were typically ignored in the past studies. This poses a question about the influence of column base condition on the seismic performance and stability of such columns, which has not been well comprehended yet. This paper aims at examining the nonlinear response of the steel wide-flange columns including the base connection under seismic-induced demands. Once the corroborated finite element model of the column isolated from a five-storey steel MRF is developed including its base connection, footing, and the flexibility of storey beams, the history of the axial load, rotation and displacement demands obtained from a nonlinear response time history analysis of the frame under a representative earthquake ground motion acceleration are imposed to the column FE model. The results obtained from the analysis of the column with base connections are then compared to those featuring an identical column, but with fixed base and flexible top end condition to characterize the effect of column base connection on the seismic response of MRFs with exposed base plates.

2 Description of Experimental Database

In this study, the experimental program performed by Gomez et al. [15] who examined the seismic performance of exposed column base connections under axial compression and flexure was selected to develop and verify the numerical model of the wide-flange column with the base connection. The experimental test setup is presented in Fig. 1. This test program involved testing seven large-scale column base connections with W8 × 48 columns with flange width-to-thickness ratio of 5.92 and web width-to-thickness ratio of 21.25, welded to the centre of the base plate with partial

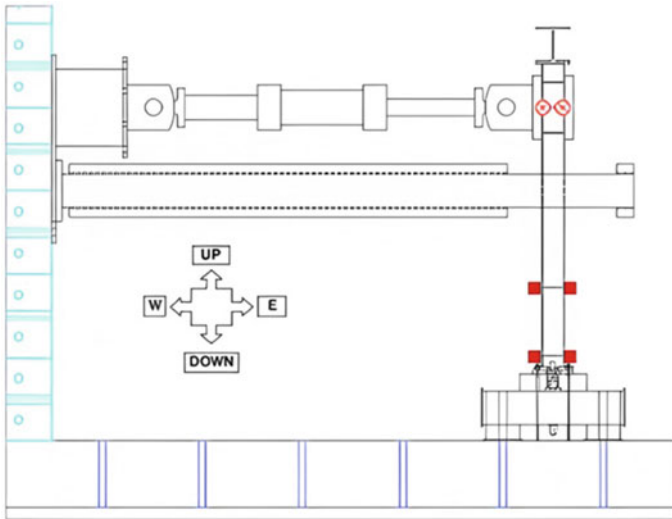


Fig. 1 Experimental test setup by Gomez et al. [15]

joint penetration welds plus reinforcing fillet welds. The base plates measured 355×355 mm and three different thicknesses were studied: 25.4, 38.1, and 50.8 mm. The anchor rods were ASTM F1554 Gr. 36 or Gr. 105 with a diameter of 20 mm. The depth of the grout pad and concrete footing were 50.8 and 609.6 mm, respectively, in all the tests. The column height was 2.35 m measured from the upper side of the base plate, which approximately represents 2/3 of the height of a typical first-storey column in steel MRFs. The column was oriented such that the applied lateral displacement imposed strong axis bending. The top end of the column was braced out of plane, and the maximum lateral displacement reached 246 mm, which corresponded to 10.6% storey drift ratio.

In the current study, Test 1 and 2 specimens, which were geometrically identical, were selected. Test 1 specimen was loaded monotonically subjected to a maximum drift ratio of 10.6%, while a linearly stepwise-incrementing cyclic displacement protocol following the SAC loading protocol [23] was used for the second specimen. No axial load was applied to the specimens. In Test 1, the response remained elastic up to a storey drift of 1% drift, followed by yielding of the plate, as revealed by flaking of the paint on the plate, and anchor rod yielding. Damage to the grout initiated at a drift ratio of 3%, leading to a drop in the flexural strength of the connection at 8% drift ratio. The weld connecting the corner of the column flange to the base plate fractured at a drift ratio of approximately 4%. The response in Test 2 was dominated by pinching due to the gap produced by yielding and cumulated permanent elongation of the anchor rods under cyclic loading. Damage in grout initiated at 2% drift ratio, leading to extensive crushing due to compressive action of base plate on grout at the end of the experiment. The anchor rods and the base plate yielded at drift ratios of 1 and 3%, respectively. The test stopped after the rupture of one the anchor rods at a

drift ratio of 7%, which led to a 56% drop in the flexural strength of the connection. It is worth mentioning that no fracture in the column to base plate welds was reported in this test. Refer to Gomez et al. [15] for additional details about the experiments.

3 Seismic-Induced Demands in Steel MRFs

3.1 MRF Design

A five-storey office building located on a Class C site (firm ground) in Vancouver, British Columbia (Seismic Category 4) was selected in this study. The plan view and elevation of the selected building are shown Fig. 2. The live and dead loads of typical floors are 4.6 kPa and 2.4 kPa, respectively, and the dead load and snow load at the roof level are 3.4 kPa and 1.64 kPa, respectively. The weight of the exterior walls was set equal to 0.6 kPa. The seismic loading was performed in accordance with the provisions of the upcoming 2020 National Building Code (NBC) of Canada [29] using the modal response spectrum analysis method. The importance factor is $I_E = 1.0$ and the higher mode factor $M_v = 1.0$. The lateral load-resisting system of the building consists of ductile MRFs in the long direction and ductile buckling-restrained braced frames (BRBFs) in the short direction (Fig. 2). One of the two MRFs was designed for this study. The ductility-related and overstrength-related force modification factors of the ductile MRF are $R_d = 5.0$ and $R_o = 1.5$. The period of the first mode of vibration of the MRF is 2.1 s. The seismic weight of the structure is 18883 kN which led to a total lateral seismic load of 951 kN for strength design and 632 kN for the lateral deflection check.

The MRF was designed in accordance with the seismic provisions of the Canadian steel design standard S16-19 [5]. The beams and columns are made of ASTM A992 wide-flange sections with specified and expected yield strengths of F_y 345 MPa and $R_y F_y$ 385 MPa, respectively. The modulus of elasticity of steel is $E = 200$ GPa. Further details about the design of steel MRFs can be found in [21].

3.2 Design of Column Base Plate

The exposed column base connection for the interior MRF column studied here (Fig. 2a) was designed in accordance with AISC steel design Guide 1 [14] and CSA S16-19 [5]. The detail of the base plate is shown in Fig. 3. The base plate is made of ASTM A572 Gr. 50 steel and is 88.9 mm-thick. Washer plates are also made of the same steel material with 12.7 mm thickness. In total, there are eight anchor rods, 38.1 mm in diameter and made of F1554 Gr. 105 steel. It is assumed that a shear lug welded underneath the base plate carries the shear force induced in the base connection and anchor rods are only designed under tension. The embedment

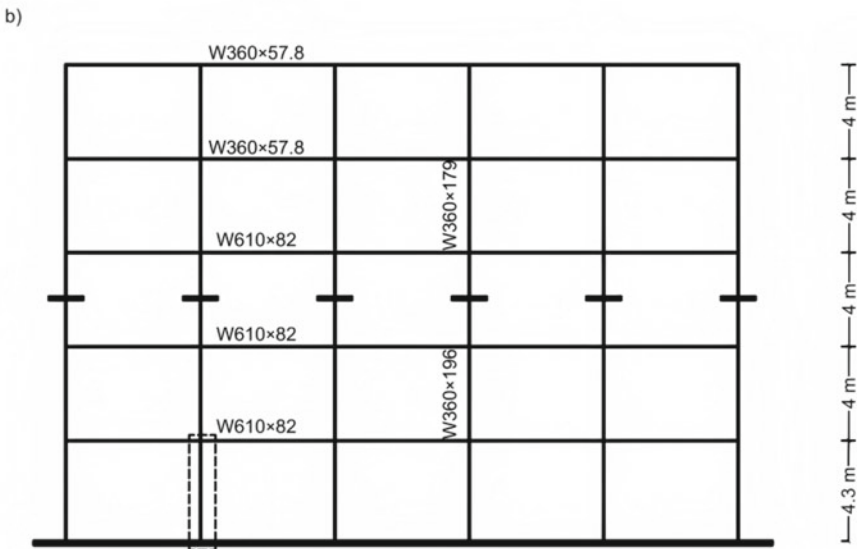
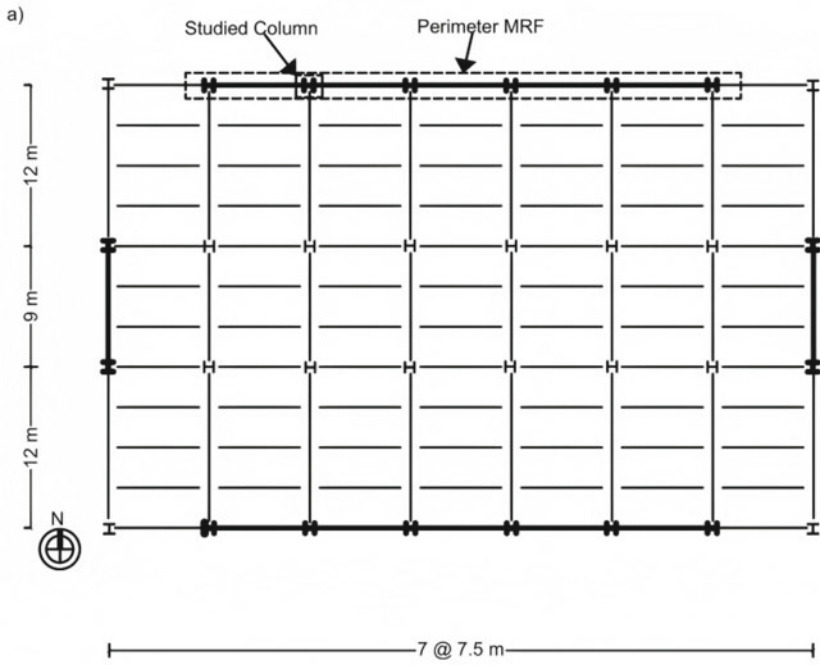


Fig. 2 Selected five-storey building **a** plan view, **b** prototype steel MRF

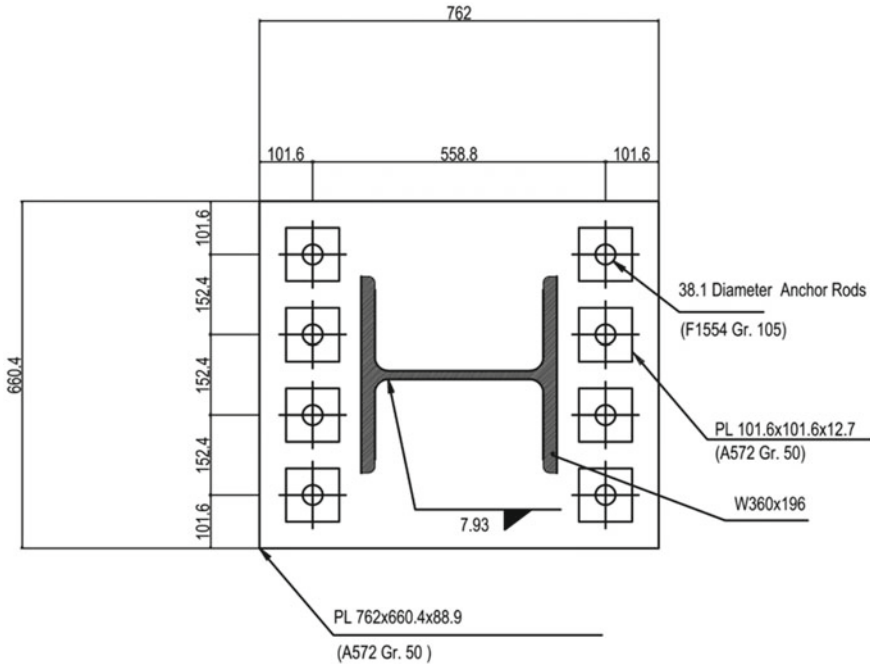


Fig. 3 Details of the column base plate (dimensions in mm)

length of the anchor rods is limited to one metre, benefitting supplemental shear reinforcement for restraining concrete breakout.

3.3 Concentrated Plasticity-Based Model

A two-dimensional (2D) model of the selected MRF (Fig. 2b) was constructed in OpenSees using nonlinear zero-length springs assigned at the ends of beams and columns plus elasticBeamColumn elements joining their end springs. The nonlinear cyclic properties of zero-length springs were based on the Ibarra Medina Krawinkler (IMK) deterioration model [27]. The nonlinear response of the IMK springs assigned to the column bases was modified as recommended by [26] to account for the influence of the column axial force and end conditions on its cyclic response. The panel zone was modelled using the parallelogram model with a nonlinear trilinear flexural spring along with rigid elements [16]. The columns were assumed to be fixed at their bases. A leaning column made of truss elements with relatively high axial stiffness was included to impose P-Delta effects from the gravity columns tributary to the selected MRF. That column was connected to the MRF at each storey using a relatively rigid truss element to simulate a rigid floor diaphragm response. Lumped

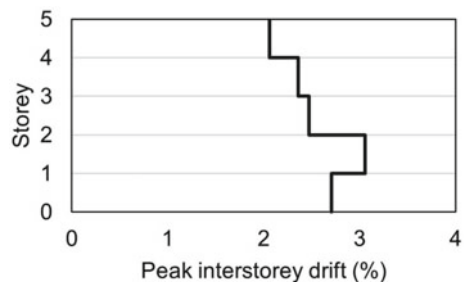
masses were assigned to the top nodes of the columns to reproduce the seismic mass of the building associated with the MRF. The Rayleigh damping method with mass and stiffness proportional damping corresponding to a critical damping ratio of 2% in the first and second vibration modes was used to reproduce the classical damping matrix of the structure [37]. Refer to [21] for additional details regarding the concentrated plasticity-based model of the MRF.

In a well-designed MRF, out of plane bracing through floor slab or point bracing is provided to the beam which ensures that the weak axis flexure remains almost elastic. The modelling approach in which elastic properties are assumed for weak axis flexure of MRF beams should not significantly influence the in-plane response of the frame examined in this paper. In this context, 2D frame analysis is sufficient to obtain displacement demands at top of the column which is subsequently imposed in detailed 3D finite element analysis.

3.4 First-Storey Column Deformation Demands

Nonlinear Response History Analysis (NLRHA) of the MRF was performed under the 2003 Tokachi-Oki, Kitami N-S, interface subduction earthquake record scaled to match the design response spectrum for the site following the guidelines of the NBC Commentary J. Under the selected ground motion record, no collapse was observed, and the profile of the peak storey drifts over the frame height is shown in Fig. 4. In the first-storey, the maximum inter-storey drift reached 2.7%. The time histories of horizontal displacement and rotation at the top of the selected first-storey interior column are presented in Fig. 5a, b, respectively. As indicated, these results were obtained assuming fixed base conditions for the columns.

Fig. 4 Profile of peak storey drift ratios



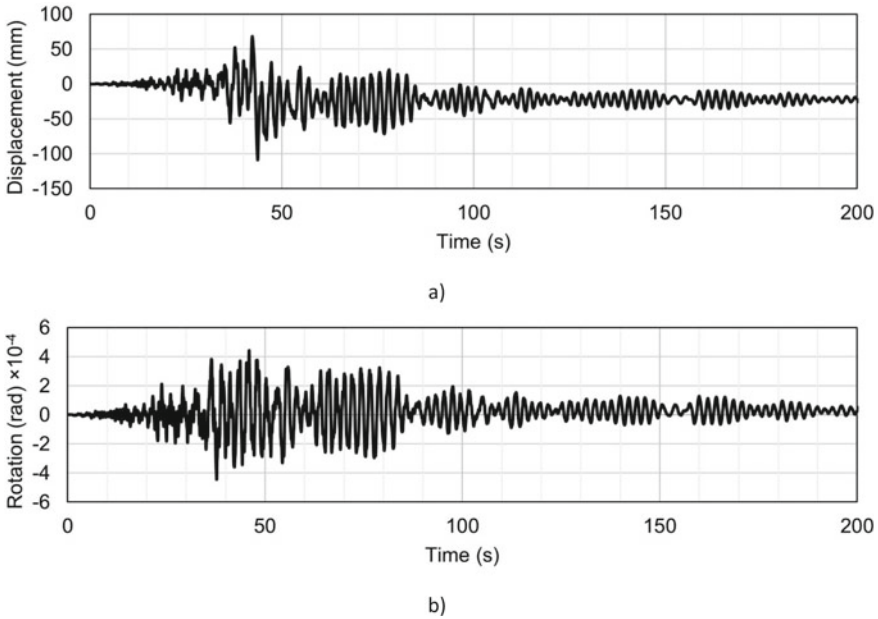


Fig. 5 Seismic-induced demands at top of the interior first-storey column under the 2003 Tokachi-Oki, Kitami N-S earthquake: **a** in-plane displacement history, **b** strong axis rotation history

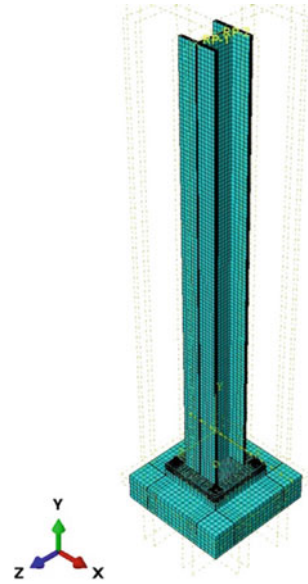
4 Influence of MRF Column Base Conditions on the Column Response

4.1 Finite Element Model Development

The detailed three-dimensional (3D) model of the exposed column base connection was created in the ABAQUS program [1]. The finite element model of the column is shown in Fig. 6. In the model, footing, base plate, anchor rods, and columns were constructed using solid hexahedral (C3D8R) elements to explicitly simulate the thickness of base plate, grout pad, concrete pedestal, and column flanges. A total of almost 60,000 elements were used. The wide-flange column can also be made of Shell S4R elements to reduce computational cost while properly capturing local buckling. The base nodes of the column were tied in all degrees-of-freedom (DOFs) to the base plate nodes at the intersection of the column and base plate. All nuts were tied to the washers, and the washers themselves were tied to the anchor rods. The base of the footing was fixed in all DOFs, while the top end of the column was braced against out of plane deformation.

The numerical surface-to-surface contact properties having tangential and normal behaviour was used to simulate the interaction between the components of the column base connection and footing. The contact properties included steel to steel, steel to

Fig. 6 Detailed finite element model of the column and base connection



concrete, anchor rods to concrete, anchor rods to grout, and anchor rods to base plate. In steel-to-steel contact, hard contact was defined with tangential behaviour and isotropic friction using the penalty method with the coefficient of friction of 0.8. Note that hard contact definition allows for separation, which is expected between the washers and the base plate, as was observed in the test program by Gomez et al. [15]. The coefficient of friction in steel to concrete contact was assumed as 0.45. Steel-to-steel contact was used between the top washer and the base plate, as well as between the bottom washer and the base plate. Steel-to-concrete contact was considered between the base plate and the grout and between the bottom washer and the grout. Interaction between the anchor rods and the concrete, grout, and base plate was simulated using a soft contact with the linear formulation. The elastic stiffness (E) of concrete, grout, and steel were used as contact stiffness for anchor rods to concrete, anchor rods to grout, and anchor rods to base plate contact properties, respectively. The tangential behaviour of the anchor rods to concrete and anchor rods to grout contact properties was ignored, which is consistent with the observation by Gomez et al. [15]. The tangential behaviour of anchor rods to concrete and anchor rods to grout was therefore ignored in the model owing to the fact that anchor rods tend to de-bond from concrete at the beginning of loading in the test as reported by Gomez et al. [15]. The tangential behaviour of the anchor rods to base plate was also ignored. This assumption aligns with the design assumptions as the size of the anchor rod holes exceeds the anchor rod diameter, which will eliminate friction between the sides of anchor rods and the base plate.

Material nonlinearity in the base plate steel was incorporated through the Maxwell–Huber–Hencky–von Mises yield criterion with associated flow rule. The nonlinear cyclic behaviour of the steel material was reproduced using the Voce and

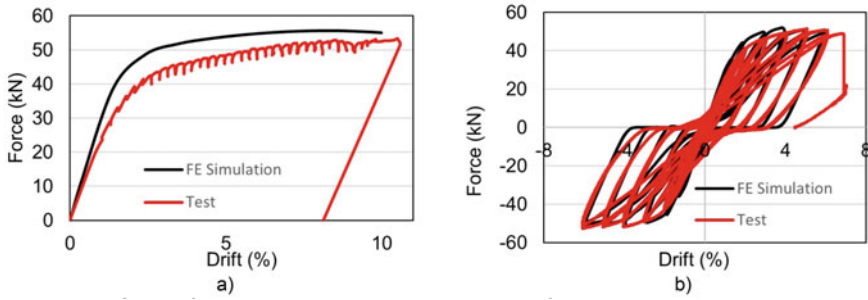


Fig. 7 Column force–displacement responses obtained from the experiment as compared to numerical predictions: **a** test 1 and **b** test 2

Chaboche plasticity model that features combined isotropic/kinematic hardening [6, 11, 17] with three back stress curves to match the ancillary test data provided by Gomez et al. [15]. Concrete and grout materials were assumed to remain elastic for simplicity and were modelled using the modulus of elasticity reported by Gomez et al. [15], i.e. $E_c = 24.13 \text{ kN/mm}^2$ and $E_g = 20.68 \text{ kN/mm}^2$, respectively [32].

4.2 Model Validation

In Fig. 7a, b, the force—displacement responses obtained from the FE model for Test 1 and 2 specimens are compared to those measured in the experimental program. Overall, very good correlation could be obtained between the predictions and the test results. The pinching response in the cyclic response (Fig. 7b) is mainly attributed to the cumulated permanent elongation of anchor rods, which prevented them from being engaged in tension after each load reversal until the base plate became in contact with the washer and nut. The elongation of the anchor rods during load reversal is illustrated in Fig. 8. Crushing of the grout was ignored in the model, as the grout was only assigned linear elastic response. However, this assumption had minor impact on the magnitude of the forces in the monotonic and cyclic tests because the force–displacement response of the column was dominated by the anchor rod and base plate yield mechanisms.

4.3 Column Response

The horizontal displacement and rotation time histories of Fig. 5 were applied at the top end of the finite element model of the selected interior first-storey column for two base conditions: fully fixed and with the base connection of Fig. 3. No global instability of the column was observed in the analyses. The comparison of

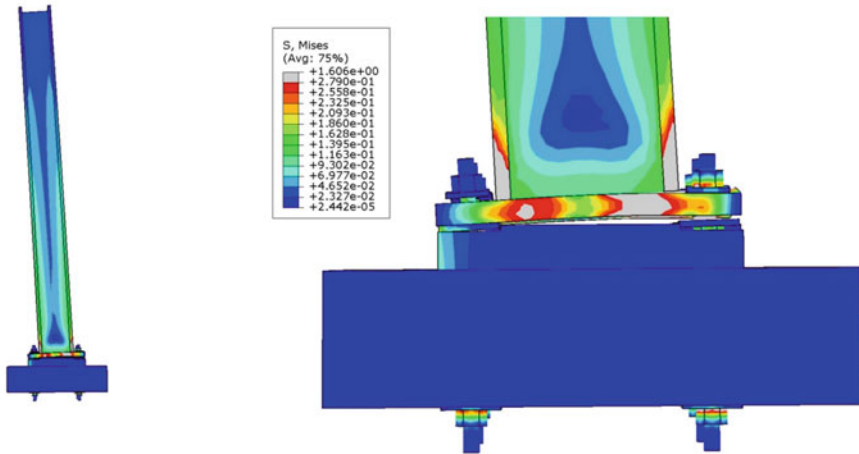


Fig. 8 Deformed shape and von Mises stress distributions of the column base at 7% drift ratio showing the elongation of the anchor rods during the load reversal under cyclic loading protocol (stresses are in kN/mm^2 ; grey zones represent yielding)

the lateral force—chord rotation and base moment—chord rotation responses of the columns with fully fixed base condition and with the base connection are presented in Fig. 9a, b, respectively. The flexural stiffness of the column with the realistic base condition is approximately 30% lower than that of the column with fully fixed condition. Moreover, the nonlinear response of the column was significantly affected when more realistic base condition was considered. In particular, limited nonlinear response was observed and column flexural yielding was limited to only few large drift excursions experienced during the ground motion. This behaviour can stem from the flexibility induced by the flexural yielding of the base plate and the plastic elongation of the anchor rods.

The deformed shape and von Mises distributions of the columns with fully fixed and realistic base conditions at the maximum drift ratio (2.7%) are shown in Figs. 10 and 11. As shown, although the extend of flexural yielding is almost the same, less severe local buckling at the base plastic hinge location accompanied by lower axial shortening was observed when realistic base conditions were considered.

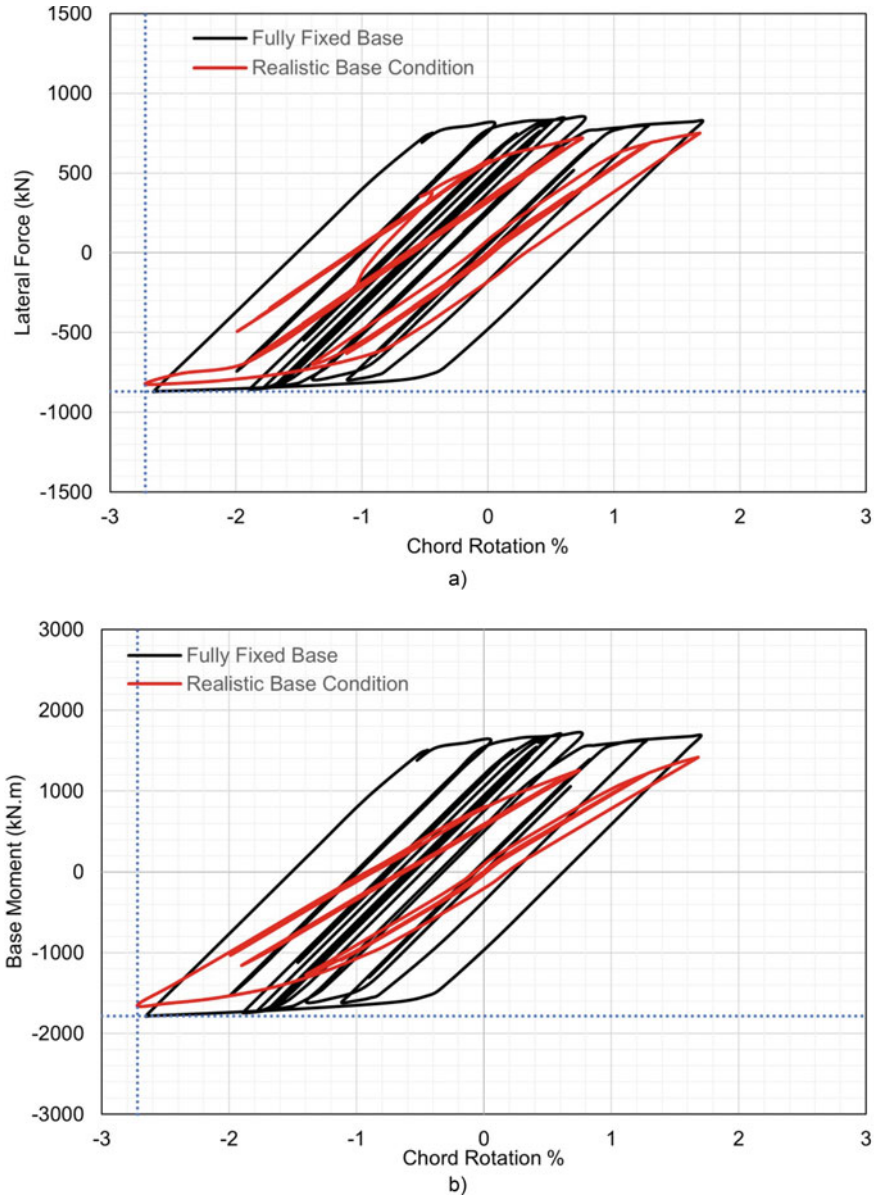


Fig. 9 Responses of the column with fully fixed base condition and the column with realistic base condition under the 2003 Tokachi-Oki, Kitami N-S earthquake: **a** lateral force—chord rotation, **b** base moment—chord rotation

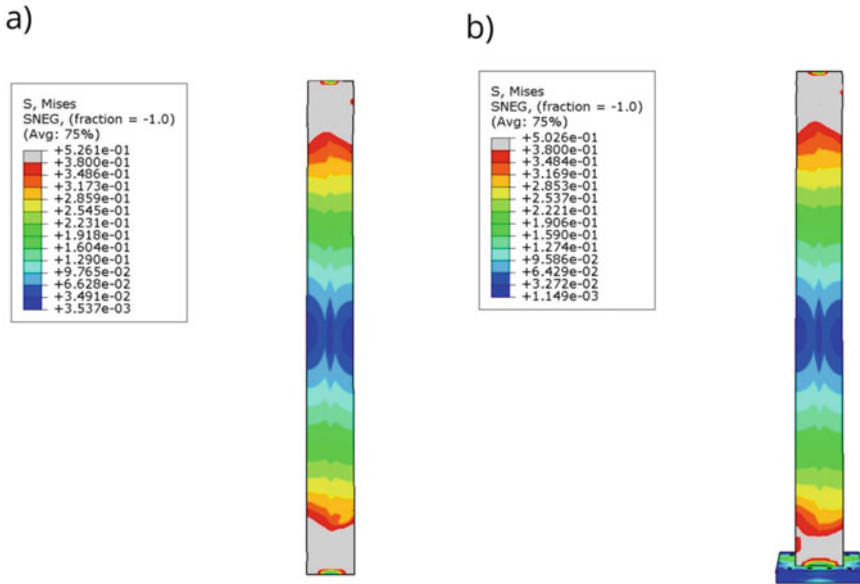


Fig. 10 Deformed shape and von Mises stress distributions of the interior first-storey MRF column at 2.7% drift ratio under the 2003 Tokachi-Oki, Kitami N-S earthquake looking at the column web: **a** column with fully fixed base condition, **b** column with realistic base condition

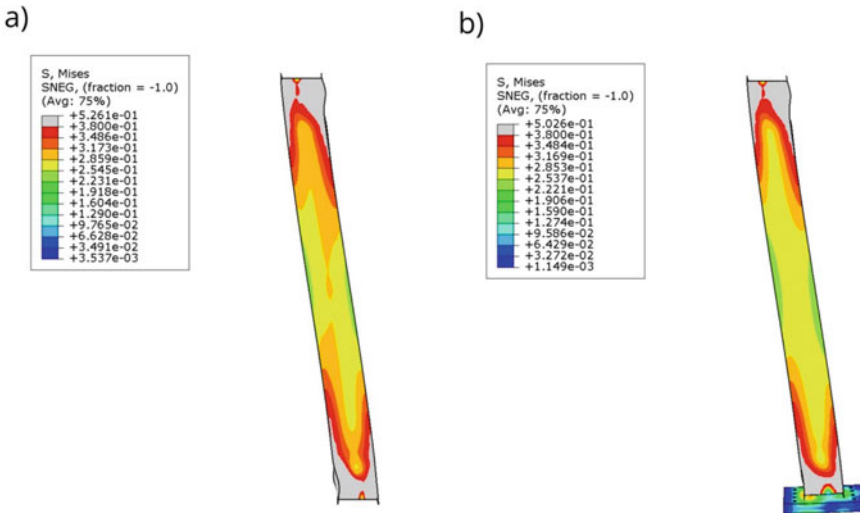


Fig. 11 Deformed shape and von Mises stress distributions of the interior first-storey MRF column at 2.7% drift ratio under the 2003 Tokachi-Oki, Kitami N-S earthquake looking at the column flange: **a** column with fully fixed base condition, **b** column with realistic base condition

5 Conclusion

The objective of this study was to evaluate the effect of the column base conditions on the nonlinear cyclic response of steel wide-flange columns with exposed column base connections located in the first storey of steel ductile MRFs. A detailed finite element model of the column and its base connection was developed in ABAQUS and calibrated against past experimental test data. The nonlinear cyclic response of the columns with a fully fixed base condition and with realistic base connection condition was examined under seismic-induced demands obtained from NLRHA of the MRF subjected to a ground motion record from a severe interface subduction earthquake. The key findings of this study can be summarized as follows:

- A detailed continuum-based finite element model of an MRF column base including the base plate, anchor rods, grout, and footing concrete was developed and tied to the first-storey column shell-based model to study the column cyclic response taking into account realistic base conditions. Numerical modelling recommendations were proposed.
- The experimentally observed pinching response of exposed column base connections due to cumulated permanent elongation of the anchor rods could be accurately reproduced using the proposed numerical model.
- The cyclic inelastic response of the exposed column base connection is mainly controlled by yielding of the anchor rods and the base plate.
- Realistic base conditions that account for the deformations of the base plate, anchor rods, grout, and footing concrete can significantly affect the nonlinear cyclic response and the severity of local buckling of wide-flange columns located in the first storey of steel MRFs.
- The flexural stiffness of the column was reduced by approximately 30% when considering realistic base conditions. Moreover, the magnitude of the flange and web local buckling at the base plastic hinge locations appreciably decreased.
- Realistic base conditions can significantly affect the displacement response of the first storey of MRFs and the demand on the columns in that storey under seismic loading.

Future studies should evaluate the flexibility of the column base for deeper wide-flange columns preferred in the construction of steel MRFs. Moreover, realistic base conditions of wide-flange MRF columns should be factored in when analysing the structural response under seismic loading.

Acknowledgements Financial support provided by the Natural Sciences and Engineering Research Council (NSERC) of Canada and the Canadian Institute of Steel Construction (CISC) is acknowledged.

References

1. Abaqus G (2020) Abaqus 6.14.1. Dassault Systemes Simulia Corporation, Providence, RI, USA
2. Astanteh A, Bergsma G, Shen JH (1992) Behavior and design of base plates for gravity, wind and seismic loads. In: Proceedings of the national steel construction conference, 209–14. AISC Chicago, IL
3. Bajer M, Vild M, Barnat J, Holomek J (2014) Influence of selected parameters on design optimization of anchor joint. In: 12th international conference on steel, space and composite structures, pp 28–30
4. Burda JJ (1999) Studies of seismic behavior of steel base plates. University of Nevada, Reno
5. Canadian Standards Association (2019) CSA S16: 19. Design of Steel Structures, Toronto, Canada
6. Castro e Sousa AD, Suzuki Y, Lignos D (2020) Consistency in solving the inverse problem of the voce-chaboche constitutive model for plastic straining. *J Eng Mech* 146 (9):04020097
7. Choi J-H, Ohi K (2005) Evaluation on interaction surface of plastic resistance for exposed-type steel column bases under biaxial bending. *J Mech Sci Technol* 19(3):826–835
8. Cloete R, Roth CP (2021) Column base connections under compression and biaxial moments: experimental and numerical investigations. *J Constr Steel Res* 184:106834
9. DeWolf JT, Sarisley EF (1980) Column base plates with axial loads and moments. *J Struct Div* 106(11):2167–2184
10. Elkady A, Güell G, Lignos DG (2020) Proposed methodology for building-specific earthquake loss assessment including column residual axial shortening. *Earthquake Eng Struct Dynam* 49(4):339–355
11. Elkady A, Lignos DG (2015) Analytical investigation of the cyclic behavior and plastic hinge formation in deep wide-flange steel beam-columns. *Bull Earthquake Eng* 13(4):1097–1118
12. Elkady A, Lignos DG (2018) Full-scale testing of deep wide-flange steel columns under multi-axis cyclic loading: loading sequence, boundary effects, and lateral stability bracing force demands. *J Struct Eng* 144(2):4017189
13. Fahmy M, Stojadinovic B, Goel SC (1999) Analytical and experimental behavior of steel column bases. In: Proceedings of 8th Canadian conference on earthquake engineering. Canadian Association for Earthquake Engineering, Ottawa, ON, Canada
14. Fisher JM, Kloiber LA (2006) Steel design guide 1-base plate and anchor rod design. AISC, pp 801–806
15. Gomez I, Deierlein G, Kanvinde A (2010) Exposed column base connections subjected to axial compression and flexure
16. Gupta A (1999) Seismic demands for performance evaluation of steel moment resisting frame structures. Stanford University
17. Hartloper AR, de Castro e Sousa A, Lignos DG (2021) Constitutive modeling of structural steels: nonlinear isotropic/kinematic hardening material model and its calibration. *J Struct Eng* 147(4):04021031
18. Inamasu H, Kanvinde AM, Lignos DG (2019) Seismic stability of wide-flange steel columns interacting with embedded column base connections. *J Struct Eng* 145(12):04019151
19. Inamasu H, Lignos DG (2022) Finite element modeling and behavior of dissipative embedded column base connections under cyclic Loading. *J Constr Steel Res* 189:107063
20. Inamasu H, Lignos D, Kanvinde A (2018) Influence of embedded steel column base strength on earthquake-induced residual deformations. In: Proceedings of the 16th European conference on earthquake engineering
21. Islam A, Imanpour A (2022) Stability of wide-flange columns in steel moment-resisting frames: evaluation of the Canadian seismic design requirements. *Bull Earthquake Eng*: 1–27
22. Kanvinde AM, Grilli DA, Zareian F (2012) Rotational stiffness of exposed column base connections: experiments and analytical models. *J Struct Eng* 138(5):549–560
23. Krawinkler H, Gupta A, Medina R, Luco N (2000) Development of loading histories for testing of steel beam-to-column assemblies. Stanford University

24. Lee D-Y, Goel SC, Stojadinovic B (2008a) Exposed column-base plate connections bending about weak axis: I. Numerical parametric study. *Int J Steel Struct* 8(1):11–27
25. Lee D-Y, Goel SC, Stojadinovic B (2008b) Exposed column-base plate connections bending about weak axis: II. Experimental study. *Int J Steel Struct* 8(1):29–41
26. Lignos DG, Hartloper AR, Elkady A, Deierlein GG, Hamburger R (2019) Proposed updates to the ASCE 41 nonlinear modeling parameters for wide-flange steel columns in support of performance-based seismic engineering. *J Struct Eng* 145(9):04019083
27. Lignos DG, Krawinkler H (2010) Deterioration modeling of steel components in support of collapse prediction of steel moment frames under earthquake loading. *J Struct Eng* 137(11):1291–1302
28. Myers AT, Kanvinde AM, Deierlein GG, Fell BV (2009) Effect of weld details on the ductility of steel column baseplate connections. *J Constr Steel Res* 65(6):1366–1373
29. National Research Council (2020) User's guide—NBC 2020 structural. Canadian Commission on Buildings and Fire Codes, National Research Council of Canada
30. Pan J, Huang R, Xu J, Wang P, Wang Z, Chen J (2021) Behavior of exposed column-base connections with four internal anchor bolts under seismic loading. *Structures* 34:105–119
31. Seco LD, Silva MC, Hjjaj M, Neves LC (2021) Column base-plates under biaxial bending moment. *Eng Struct* 231:111386
32. Singh G, Woods J (2022) 2D and 3D numerical modelling of exposed steel base plate connections under cyclic loading. *Can J Civ Eng*
33. Thambiratnam DP, Paramasivam P (1986) Base plates under axial loads and moments. *J Struct Eng* 112(5):1166–1181
34. Tremblay R, Filiatrault A, Timler P, Bruneau M (1995) Performance of steel structures during the 1994 Northridge earthquake. *Can J Civ Eng* 22(2):338–360
35. Uang C-M, Ozkula G, Harris J (2015) Observations from cyclic tests on deep, slender wide-flange structural steel beam-column members. In: *Proceedings of the SSRC annual stability conference*
36. Zareian F, Kanvinde A (2013) Effect of column-base flexibility on the seismic response and safety of steel moment-resisting frames. *Earthq Spectra* 29(4):1537–1559
37. Zareian F, Medina RA (2010) A practical method for proper modeling of structural damping in inelastic plane structural systems. *Comput Struct* 88(1–2):45–53